Stable combustion under carbon dioxide enriched methane blends for Exhaust Gas Recirculation (EGR)

Aniekan Okon[a], Osvaldo Vigueras-Zuniga[b], Ogbonnaya Agwu[a,c], Cheng Tung Chong[d], Agustin Valera-Medina[c]

[a]Department of Mechanical Engineering, University of Uyo, Uyo, Nigeria

[b]Department of Mechanical Engineering, Universidad Veracruzana, Veracruz, Mexico

[c]College of Physical Sciences and Engineering, Cardiff University, Queen's Building CF243AA, UK.

[d]China-UK Low Carbon College, Shanghai Jiao Tong University, Lingang, Shanghai 201306, China.

Abstract

Exhaust gas recirculation (EGR) is one of the main techniques to enable the use of oxyfuel combustion for carbon capture and storage (CCS). However, the use of recirculated streams with elevated carbon dioxide poses different challenges. Thus, more research is required about the cumulative effects on the desirable outcomes of the combustion processes such as thermal efficiency, reduced emissions and system operability, when fuels with high CO_2 concentration for CCS exhaust gas recirculation or biogas are used. Therefore, this study evaluates the use of various CO_2 enriched methane blends and their response towards the formation of a great variety of structures that appear in swirling flows, which are the main mechanism for combustion control in current gas turbines systems. The study uses 100 kW acoustically excited swirl-stabilised burner to investigate the flow field response to the resultant effects of the variation in the swirl strength, excitation under isothermal condition and the corresponding effects during combustion with different fuels at various CO_2 concentrations. Results show changes in size and location of flow structures as a result of the changes in the mean and turbulent velocities of the flow field, consequence of the imposition of different swirl and forcing conditions. Improved thermal efficiency is also observed in the system when using high swirl and forcing while the blend of CO_2 with methane balanced the heat release fluctuation with a corresponding reduction in the acoustic amplitudes of the combustion response, suggesting that certain CO_2 concentrations in the fuel can provide more stable flames. Concentrations between 10 to 15% CO_2 volume show great promise for stability improvement, with the potential of using these findings in larger units that employ CCS technologies.

Keywords: Thermoacoutics, swirl, coherent structures, carbon dioxide fuel blends, stability.

1. Introduction

Most gas turbine systems run under lean conditions using swirling flows. Nevertheless, this injection and flow stabilisation technique is susceptible to combustion instabilities, self-excited combustion driven oscillations that appear as a result of the coupling between the unsteady heat release and the combustor's dynamic pressure [1-3]. The flow, flame and pressure fields are all synchronised such that

a disturbance in one field spreads to other domains. These oscillations reduce the thermal efficiency of the system, wearing-out components and potentially liberating hot pieces into the flow stream in extreme cases.

A common technique to stabilise flame in the combustion zone of a burner is the use of swirling flows. It provides a mechanism which generates coherent flow structures characterized by high shear stress and turbulence needed to stabilize the flame [4-5]. The swirl strength of the flow is characterised by the swirl number, S, which is given as,

$$S = \frac{G_\theta}{G_x r} \quad (1)$$

Where G_θ , G_x, r are the axial flux of angular momentum, the axial flux of axial momentum and nozzle radius respectively [6].

Under specific swirl conditions, a vortex breakdown, a sudden change in the vortex core due to the baroclinic transitions from subcritical to supercritical conditions, appears in the flow field, eventually leading to the development of what is known as the Central Recirculation Zone (CRZ) [7], one of many large-scale coherent structures in these flows. This recirculation zone is characterized by reversed flows with local stagnation points, a mechanism which mixes the hot combustible gases with the incoming fresh mixture, thus providing flame anchorage and stability.

Moreover, the high velocity jet exiting the injector creates a differential with the ambient air flow, thereby developing shear layers. Within this region, large flow structures are generated and moved downstream of the combustion zone as a result of the Kelvin-Helmholtz (K-H) instabilities [7]. These resulting structures are convected into the flame zone with the alteration of the flame front at a specific time lag resulting in the oscillation in heat release rate, a critical determinant of the dynamic pressure oscillations within the combustor. Thus the swirl number has a substantial control on the flow, flame and pressure fields through the establishment of jet and coherent structures that impact on the entire flow field.

If that was not enough, external excitation also influences the flow profile. For example, forcing of the flow as a result of vibrations in the feed lines, or structural components can also alter the flame behaviour and retro-feeding of heat released towards the flame. In order to study these effects, many studies have been conducted on the area of thermoacoustic combustion. One example is the work of Cohem and Hibsman, who with a discrete sinusoidal frequency changed the injection patterns on a swirl injector, with corresponding cyclic fluctuation of mass flow rate as illustrated in equation (2), [8],

$$\dot{m} = \dot{m}_0 [1 + \propto \sin(2\pi f_0 t)] \quad (2)$$

where $\dot{m}_0$ denotes the mean mass flow and f_0 the forcing frequency. The flow and flame oscillation frequencies are sometimes assumed to be same as the forcing frequency [9]. Thus the excitation of the

flow field oscilates the mass flow, varies the velocity profiles and convects them to the flame zone resulting in heat release oscillation.

Finally, heat release fluctuations are also affected by the chemical time scale as a result of fuel composition. Modern gas turbines use natural gas due to its enhanced thermal efficiency, cost effectiveness, and environmental friendliness. However, techniques such as Carbon Capture and Storage (CCS) via Exhaust gas recirculation (EGR) for oxy-fuel combustion require blending the base fuel (natural gas) with gases like carbon dioxide [10]. The concept is based on increasing the carbon dioxide content of the outflow products, thus raising the efficiency of capture of CO_2. However, these blends alter the chemical kinetics of the natural gas, resulting in heat release oscillations.

By mass, the air – fuel ratio of methane is 17.16. This represents its equivalence ratio at stoichiometric combustion as given in equation 3.

$$CH_4 + 2(O_2 + 3.76N_2) \rightarrow CO_2 + 2(H_2O) + 2(3.76N_2) \quad (3)$$

The methane – air combustion is changed chemically, physically, and thermodynamically, when CO_2 is added, as illustrated in equation 4

$$CH_4 + aCO_2 + 2(O_2 + 3.76N2) \rightarrow (a+1)\ CO_2 + 2(H_2O) + 2(3.76N_2) \quad (4)$$

where a denotes the CO_2 – methane molar fraction. Although the blend of CO_2 with methane reduces the turbulent flame speed and temperature, it also reduces the formation of NOx [11-13]. This reduced flame temperature with CO_2 has a corresponding effect on its strain rate. According to Park et al. [14] the addition of CO_2 to methane-air gives a diluent effects due to the relative reduction in the concentrations of the reactive species and direct chemical effects as a result of the breakdown of CO_2 through the reactions of third-body collision and thermal dissociation. Also, the heat capacity of CO_2 and its absorption coefficient is quite high, which could alter the flame axial velocity gradient. Lewis et al. [15] experimentally demonstrated the decrease in the high momentum flow region (HMFR) velocity and increased central recirculation zone velocity with methane –CO_2 blends due to the high specific heat of CO_2 which increases the pressure differential and drives recirculation. They also showed how the imposition of swirl to these diluted blends can affect stability, thus requiring the addition of oxygen up to 30% (vol) to enable the flame anchorage to the burner. Also, Rokke [16] experimentally showed the reduction in NOx formation with methane –CO_2 blends due to the reduced temperature, while combustion stability limits were largely dependent on the mass-based additive to fuel ratio. Thus these characteristics of CO_2 are expected to have substantial effects on the flame heat release fluctuation when blended with methane.

Under more practical conditions, analyses conducted by Herraiz et al. [17] reported CO_2 concentrations in excess of 14% (vol) without major deviations in the operating parameters of a Combined Cycle (CC),

thus suggesting certain concentrations to maintain operability in Exhaust Gas Recirculation (EGR) techniques. In parallel, Gutesa-Bozo et al. [18] highlighted the need of "off-design" features in combustion and injection technologies if CO_2, in combination with other gases, is employed in gas turbine systems. However, neither of these works fully addressed the combustion parameters in swirling flames. In contrast, works by Al-Doboon et al. [19] approached the concept from the combustion point of view. Assessing numbers of blends and CO_2 concentrations, amongst other gases such as Ar and steam, the combustion characteristics of EGR imposed on a concept named "CARSOXY" showed the temperature and emissions profiles from numerical calculations in a conceptual cycle. Results denote how CO_2 in combination with Ar and steam cannot only raise efficiencies but also enable large power conditions similar to those of conventional power cycles. Furthermore, the combustion features of mixtures with high CO_2 concentrations have been partially addressed by Yilmaz and Yilmaz [20] who changing the fuel mixture and reaching up to 20% CO_2 (vol) showed that at different swirl numbers and carbon dioxide concentrations the emission profiles and temperatures in the system were not monotonous, with a great variation at different equivalent ratios. Simultaneously, works from Liu et al. [21] also denote the impact of CO_2 on flame behavior at various power outputs, with CO_2 showing the lowest temperature profiles compared to nitrogen and argon. This has clear implications not only on stability but also the formation of emissions such as thermal NOx. Also, within the study of fossil fuels, the implications of these lower temperatures demonstrated the reduction of soot formation, that although produced larger polycyclic aromatic hydrocarbons (PAHs), can lead to methods of fuel/diluent blending to mitigate emissions and unwanted pollutants for CCS technologies. However, the question of how other instabilities combined with temperature and swirl can impact on these blends is still unknown.

Regarding thermoaocustic instabilities, many studies model the flame as a function of the heat release fluctuation to the inlet velocity oscillation of the flow field, equation 5 [22-28], and used to predict acoustic-based combustion instabilities within the combustor [9, 29-30].

$$\frac{Q\prime}{\bar{Q}} = \text{FTF}\,\frac{U\prime}{\bar{U}} \tag{5}$$

Where Q' and U' are the instantaneous heat release and velocity while $\bar{Q}$ and $\bar{U}$ respectively represent their mean values. This heat release oscillation is known to be the main nonlinearity in the combustion zone, [31], as the acoustic field is energised when this heat release oscillation is in phase with the dynamic pressure of the combustor and vice versa.

However, while variation in the swirl strength and flow excitation is expected to alter the flow matrix with corresponding variation in the convective time scale, the blend of methane with CO_2 is expected to vary the chemical time scale with an overall effect on the flame heat release fluctuation and pressure dynamics within the combustor, thus altering the effect on the flame transfer functions. These parameters have not been investigated yet, and a gap of understanding their effect on flame stability still require further studies. Moreover, the change in heat release, density and impact of the fuel blend

will also affect the formation of coherent structures essential for stabilisation of the flow field, an area that has not been addressed yet by the current literature. Hence, there is now the curiosity as to whether the individual variations of these parameters could cumulatively enhance the pressure dynamics, alter the flow field and run the system in a stable condition.

2. Method

A manufactured 100kW swirl-stabilised burner was used for this experiment. An 8 Ohm loudspeaker was mounted at the bottom of the plenum to excite the flow field, figure 1.

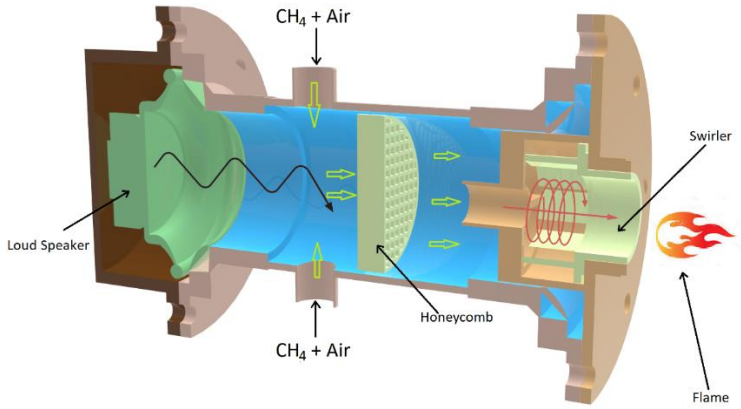

Figure 1: A schematic of the combustor

Two 40mm diameter tubes positioned opposite each other supplied air to the premixed confinement. A honeycomb was placed across the flow to remove large-scale fluctuations of flow. An 80mm diameter cylindrical injection section with three pre-swirl vanes attached to a centre bluff rod which runs throw the 28mm swirl nozzle injected air into the enclosure for the measurement of the flow dynamics by the sensors. The flame was confined from environmental ambience with a 400mm long, 84mm internal diameter quartz tube. The system was excited by a signal generator via the loudspeaker with a frequency range of 100 and 500 Hz.

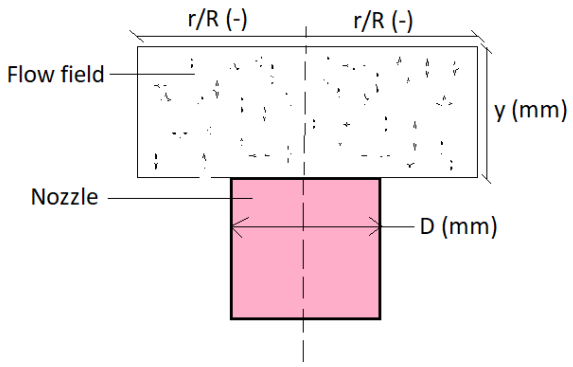

Figure 2: Isothermal flow field in the confined quartz tube and representative flame (CH4, S =1.05, Ø = 0.70).

Isothermal conditions were assessed at a mass flow rate of ~2.5 g/s and 1 bar inlet pressure. The flow field (54mm x 23mm) was normalised to the internal diameter (D) of the nozzle and to the ratio of the probe distance (r) from the centreline of the flow for the height and horizontal length, respectively.

A Flowlite Dantec Laser Doppler Anemometer (LDA) powered using the BSA Flow Software was employed for velocity data acquisition. The measurement matrix was designed to measure 621 points at 2mm vertical and 1mm horizontal steps. Count of the seeding particles, i.e. aluminium oxide, was kept at 10000, far above the minimum accuracy level of 2000 [32]. An intrusive Constant Temperature Anemometer CTA, with Stream Ware software [33] was also used to validate the flow velocity profiles from the LDA, providing a deviation of 3.2% between both systems.

Combustion experiments followed. Chemiluminescence analyses of CH* species were obtained to characterize heat release fluctuations in the system [34]. A Photron Fastcam APX-RS high-speed camera operating at 1000 frames/s with a 105 mm, 1:2.8 Nikon lens was used to measure the CH* chemiluminescence change of the studied flames. A 431nm narrow bandpass optical filter was used to allow only the CH* wavelength to pass through the optics and record only the radical formation across the field. This technique has been reported by many authors [35-37]. The results were integrated for each frame using a bespoke Matlab code. Experiments were run for different fuel conditions (CH4, CH4-10%CO_2, CH4-15%CO_2, CH4-20%CO_2 and CH4-30%CO_2), each with a fuel mass flow rate of 0.113 to 0.122g/s at an equivalent ratio of 0.7.

3. Results and Discussion

The results show the variation in the flow profiles and their corresponding influence on the flame and pressure domains at different conditions. These variations are crucial to the thermal efficiency, emission reduction and the stability of the system.

3.1 Coherent structures variations

Figure 3a shows the mean velocity profile of the lower swirl strength, which spans between the minimum and maximum values of -3.5 and 4.0 m/s respectively. While the negative velocity profiles indicate the flow recirculation along the flow axis, the positive profiles represent the jet flow region and the zero value represents the stagnation layer (shear layer) which separates the CRZ from the HMFR. Figure 3b shows the contour plots of the flow structures at a higher swirl strength with similar flow conditions. The higher swirl number posses a relative increase in the length and width of the CRZ, which encroaches slightly into the HMFR. This enlargement of the CRZ is attributed to the increased angular momentum of the higher swirl which draws more mixture to the zone with a resultant effect of enhanced mixing during combustion. This is a phenomenon well documented in the literature. A point of interest is the tilted flame shape, which is believed to appear as a consequence of the asymmetry of the swirler used to generate the 1.05 S case. Simultaneously, the 1.50 having more inlet ports, was more symmetrical in the axial direction, thus reducing the impact on the flame.

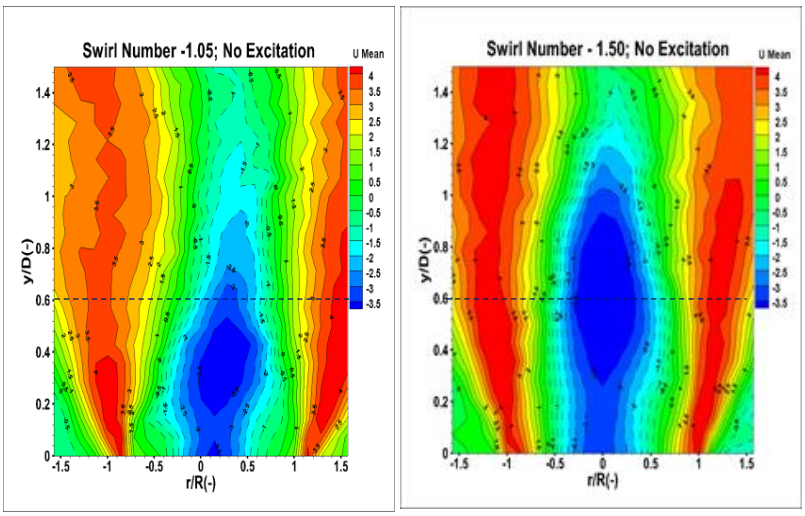

(a) (b)

Figure 3: Contour plots of vortical structure variation with Swirl Number ((a) S=1.05; (b) S= 1.50).

However, as forcing was imposed, the flow field suffered variations and the CRZ structure showed distorted patterns, Figure 4. Figure 4a shows the mean velocity profile of the lower swirl strength without external excitation. In Figure 4b, the excited flow shows some changes as a result of the periodic oscillation of the mass flow rate as a response to the external excitation, equation 2. Specifically, the shape of the CRZ is stretched and elongated while the lowest negative velocity is drawn upstream into the nozzle annulus. This change in the size of the CRZ causes a corresponding variation in the shear layers, while the highest mean velocity profiles become fragmented into separate regions. The CRZ is further elongated downstream of the flow, when the forcing frequency was increased to 200 Hz, while the fragmented structures of the HMFR become more irregular in shape. Thus with a fix swirl strength, the excitation of the flow field changes the recirculation zone with its inherent interaction with the HMFR, which are critical to the convective time scale of the flame field, thus directly affecting the stability of the flame.

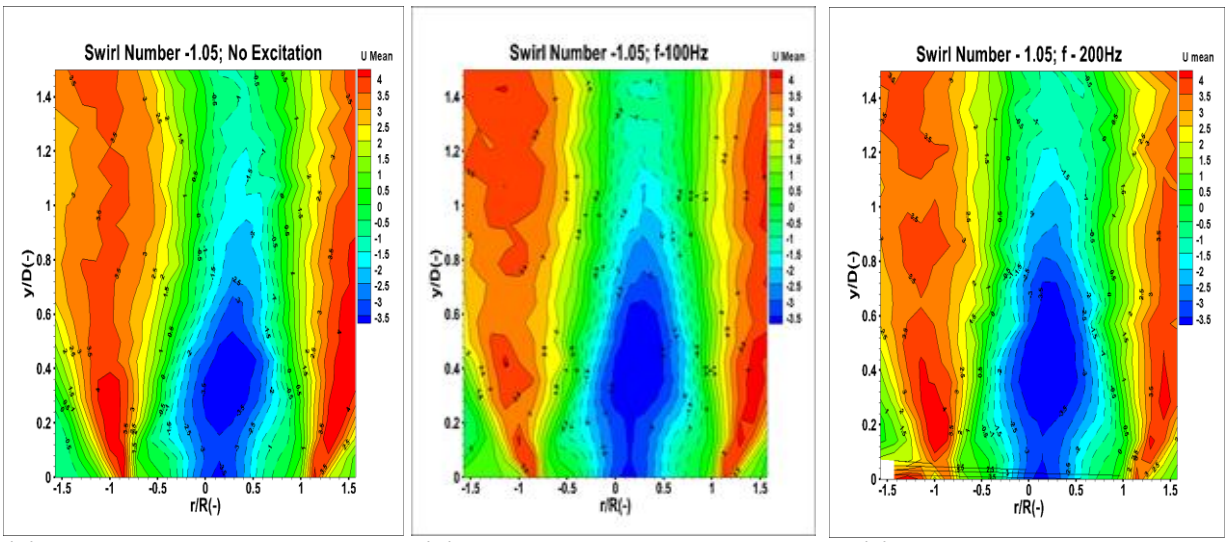

(a) (b) (c)

Figure 4: Contour plots of vortical structure variation with excitation ((a) No forcing; (b) 100 Hz; (c) 200 Hz; Units in m/s).

3.2 Combustion patterns – Fuel dependancy

Having demonstrated the effects of the variation of the swirl strength and excitation on the flow structures, corresponding effects on the heat release fluctuation with different fuels were examined. The physical and thermodynamic properties of CO_2 was thought of having a significant effect on the flame field when blended with methane. Thus the heat release oscillation rate, with reference to the variations in the swirl and fuel conditions were also investigated.

Figure 5 shows the heat release oscillations of the medium, 1.05 swirl using the 3 different blends. Comparing the three profiles, a significant change is observed between them. It is clear that the use of pure methane denotes higher fluctuations at any given flowrate, i.e. consequence of the greater heat release. Increasing CO_2 to 15% considerably decreases these heat release fluctuations, leading to greater combustion stability. Interestingly, the results fits to some previous findings by other groups [21], where carbon dioxide dilution reduced temperature profiles. Finally, an increase to 30% shows better stability than pure methane. However, it is clear that this blend is detrimental to the combustion pattern, with greater fluctuations than 15% CO_2 potentially caused by the greater dilution of the flame. Therefore, it was shown that addition of 15% CO_2 clearly makes the heat release more homogeneous and stable, while greater quantities are detrimental to flame stability, a phenomenon which might be attributed to the heat capacity and the CO_2 density compared to the other gases in the blend.

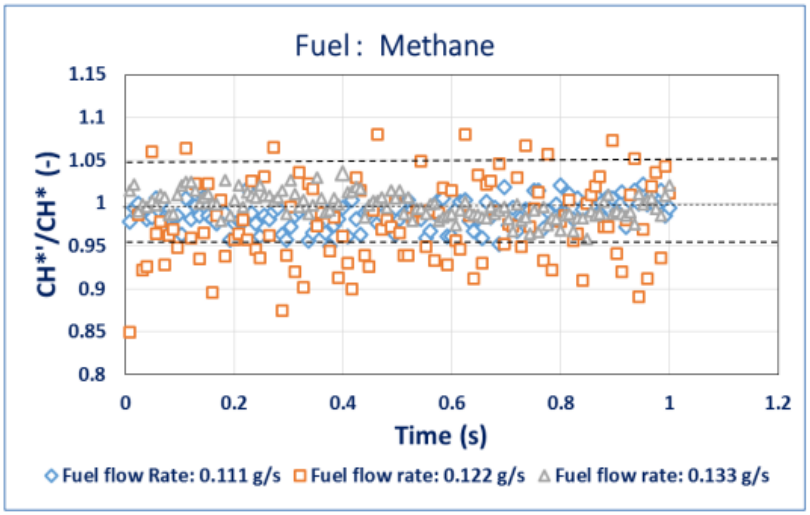

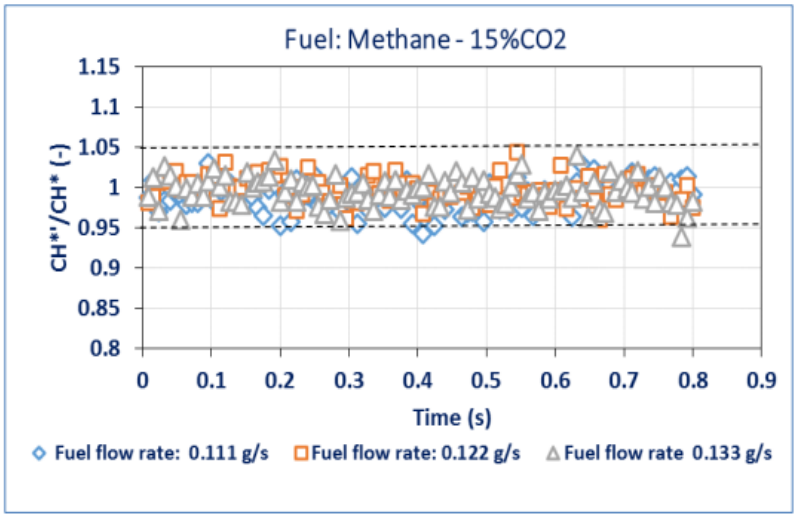

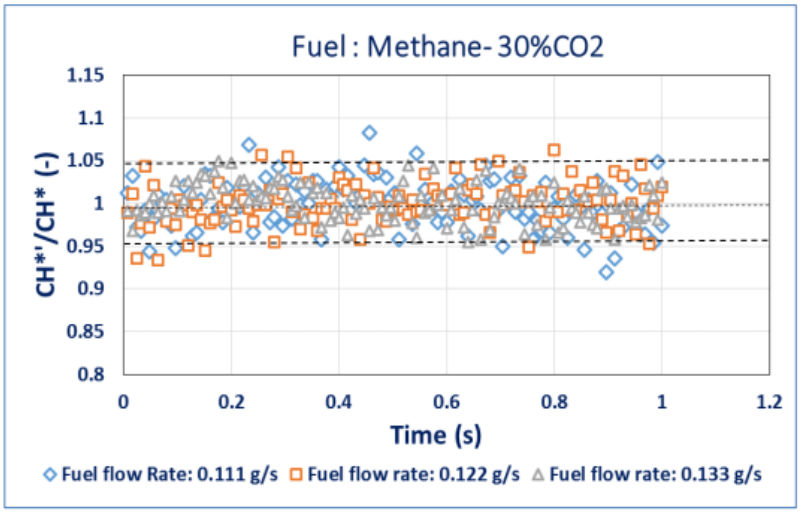

Figure 5: CH* chemiluminescence fluctuation with different CH4-CO_2 blends, (S =1.05, Ø = 0.70).

3.3 Acoustic mode dynamics with swirl and excitation conditions

Having demonstrated the impacts of the swirl number and fuel on the flow and flame fields, their corresponding influence on the combustor dynamic pressure were assessed using the pressure time series spectral analysis. The analysis relied on the variation in the amplitudes of the power spectrum. Low amplitudes denote damped acoustic modes with a lower level of system instabilities, a technique that has been documented in different studies, [2, 38- 42].

The flame enclosed with a 400mm length – 84mm diameter quartz tube open to the atmosphere recorded a natural acoustic frequency of 150 Hz. This was obtained by the Fourier Transforms (FFT) of the pressure dynamics within the flame tube. The input data for the Matlab based computation were the time series pressure oscillations. The analysis considered both swirl numbers with a constant equivalence ratio of 0.7 and an inlet velocity ratio (u'/u) of 0.3 and 0.4. The velocity ratio in this case is the ratio of the root mean square (RMS) to the bulk flow velocity. The velocity ratio was regulated by the combined effects of the fuel and air rate of flow and inlet flow pressure. In each forcing condition the dominant acoustic mode of 150Hz and the excitation frequency mode both with specific amplitudes were recorded.

Figure 6 plots the amplitudes of the acoustic modes against the excitation frequency for the low swirl strength at a velocity ratio of 0.3 and 0.4. In Figure 6a, the amplitudes of the forced modes at each excitation frequency for the two velocity ratios are presented. In most frequencies, the amplitudes remain within 0.001 kPa^2 except at 250 and 450 Hz where they stay within 0.003 kPa^2 above the benchmark at 0.002, for both velocity ratios. Figure 6b shows the corresponding natural acoustic modes for the two velocity ratios. At u'/u = 0.3, the natural mode fluctuates between the 0.002 kPa^2 margin across the excitation frequencies except at 150 Hz where it falls below 0.001 kPa^2. With an increased velocity ratio to 0.4, an increase in the acoustic amplitude is noticed above the benchmark except for the forcing frequencies at 150, 450 and 500 Hz. Therefore with a low swirl strength, most of the forced and natural modes were below and within the bench margin repectively.

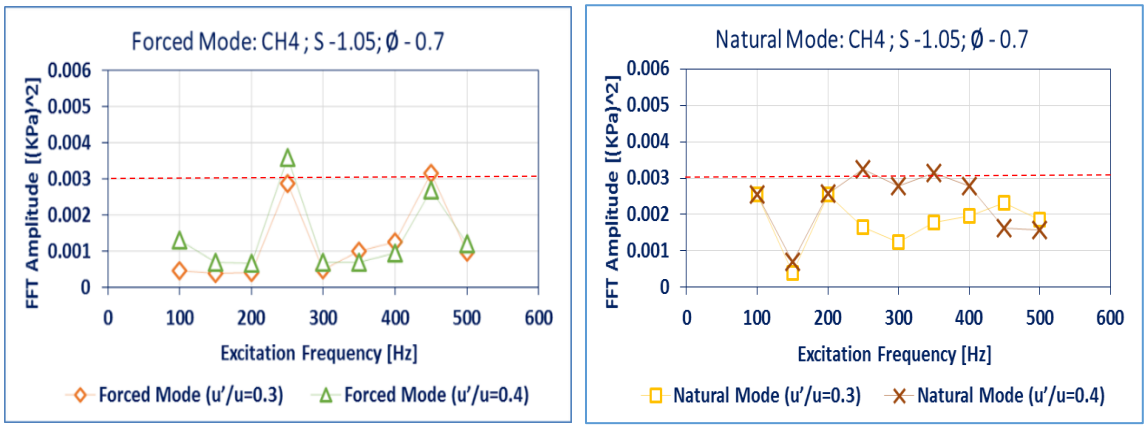

(a) (b)

Figure 6: Acoustic amplitudes of methane flame for (a) forced and (b) natural modes (S =1.05, Ø = 0.70).

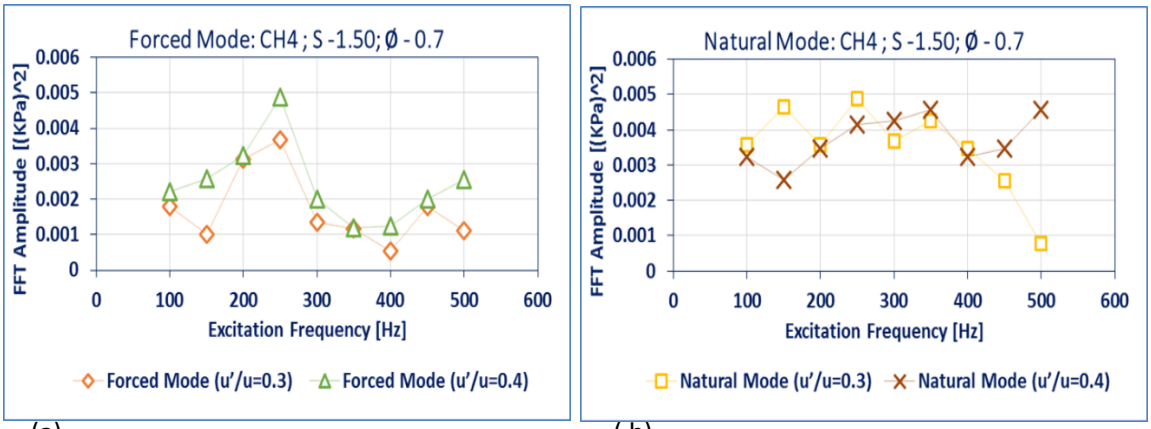

(a) (b)

Figure 7: Acoustic amplitudes of methane flame, for (a) forced and (b) natural modes (S =1.50, Ø = 0.70).

With increased swirl strength, a different phenomenon is observed, Figure 7. A significant increase in the amplitudes of the modes of both velocity ratios are evident. Most of the forced modes of lower frequencies have their amplitudes above the margin with some rising above 0.003 kPa^2 and fall below the margin at higher frequencies. The increased acoustic amplitudes became so conspicuous with the natural mode as all except three frequencies have their amplitudes above 0.003 kPa^2 . These results imply that the increased turbulence and augmented coherent structrures such as the CRZ, previously discussed, Figure 3, has culminated in an increased magnitude of the acoustic modes.

Since the increased heat release fluctuation was suppressed by the blend of methane with CO_2, the corresponding impact of carbon dioxide on the acoustic mode was thus investigated. Three percentages (10, 15 and 20%) of CO_2 were blended with methane with similar combustion condition and their acoustic amplitudes were measured and compared with those of the pure methane flames. Figures 8, 9 and 10 plot the acoustic amplitudes against the forcing frequencies of the two velocity amplitudes for methane-10%CO_2, methane-15%CO_2 and methane-20%CO_2 respectively. The methane-30%CO_2 blend was not assessed as it had already shown detrimental combustion patterns. Figure 8 plots the acoustic

modes for both swirl numbers at 1.05 and 1.50 respectively. In each case, the two velocity ratios of 0.3 and 0.4 with a fuel blend of methane and 10%CO_2 were considered. The results show a significant reduction in the amplitude of all the modes. In the lower swirl strength, except for the forced frequency of 200Hz which has its amplitudes at 0.002 kPa^2 , most amplitudes fall within 0.001 kPa^2 . A similar reduction was also evident with the higher swirl strength of 1.50 as few amplitudes fall within 0.002 kPa^2 while the rest are within 0.001 kPa^2 . When compared to the acoustic amplitudes of pure methane flames, Figures 6 and 7, the results show a considerable reduction in the acoustic amplitude as a result of the fuel blend with CO_2.

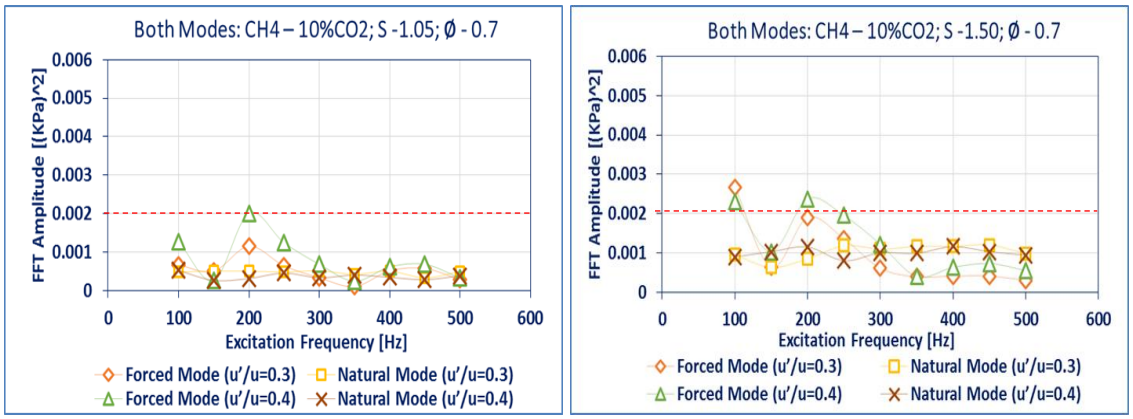

(a) (b)

Figure 8: Acoustic amplitudes of methane-10%CO_2 flame for forced and natural modes (S = 1.05, 1.50 ; Ø = 0.70).

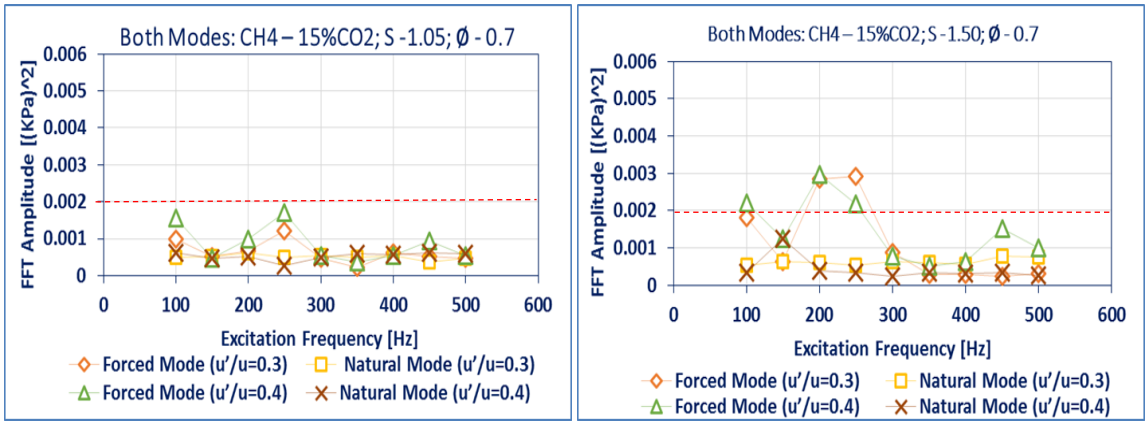

(a) (b)

Figure 9: Acoustic amplitudes of methane-15%CO_2 flame for forced and natural modes (S = 1.05, 1.50; Ø = 0.70).

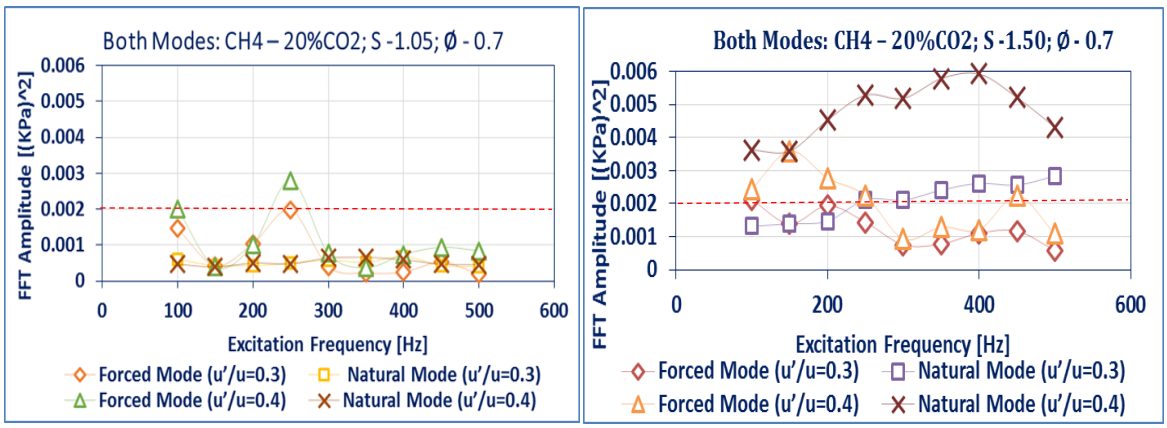

(a) (b)

Figure 10: Acoustic amplitudes of methane-20%CO_2 flame for forced and natural modes (S =1.05, 1.50; Ø = 0.70).

Increasing CO_2 further to 15%, Figure 9, denoted a similar acoustic amplitude reduction as most of the amplitudes are below 0.001 kPa^2 especially at higher frequencies while fewer amplitudes in the low frequencies are above the 0.002 kPa^2 margin. But with a 20% increase in CO_2, Figure 10, the amplitude of the forced and natural acoustic modes of the low swirl number remained low while most of the amplitudes of the higher swirl strength of 1.50 rose significantly across all the forcing frequencies.

The effects herein observed are assumed to be caused by the dilution effect of CO_2 that starts impacting on the flame front combined with a change in size of the recirculation zone. The increase in CO_2, decreases the chemical reaction timescale with the less abrupt release of heat compared to pure methane flames. Heat release, still stable, keeps the distortion of the coherent structures at low levels. However, as CO_2 is increased further and forcing distorts the cooler structures that anchore the flame and recirculate hot products, fluctuations of the flame at the particular frequencies become more accute and heat release becomes more unstable, thus increasing the noise through the system which can eventually lead to formation of holes through the flame, prior to localised blowoff and finally extinction of the combustion process. As greater swirl strength produces more elongated CRZs, the distortion becomes greater at high frequencies, considerably increasing the noise in the system under these conditions compared to the 1.05 swirl case, Figure 10.

Therefore the physical and the thermodynamic properties of CO_2 have played an important role in reducing the heat release fluctuation and its corresponding reduction in the acoustic magnitude within the combustor at certain conditions. The acoustic amplitude reduction was very effective at a low CO_2 percentages (~15%) under moderate swirl strenght (1.05). This combination of parameters needs to be evaluated at higher flowrates and pressures representative of gas turbine systems.

5.0 Conclusion

The resultant effects of swirl, forcing and fuel conditions have been asssessed in the flow, flame and the pressure fields. A higher swirl strength increased the size of the CRZ , and by extension, the flow recirculation strength. The excitation of the flow field provided further means of altering its dynamics, as the flow structures varied in shape and position with different forcing conditions, due to the periodic oscillation of the mass flow rate. All these, changed the conditions of the recirculation and mixing of the combustible mixtures resulting in the variation of the heat release fluctuations with high amplitude acoustic modes within the combustor. Nevertheless, the advantageous characteristics of CO_2 in methane blends were able to control this heat release fluctuation thus significantly reducing the amplitude of the acoustic modes. With such low amplitude acoustic modes, its growth to unstable conditions can be controlled, particularly at concentrations of CO_2 between 10 and 15% (vol). However, detrimental effects were observed at higher concentrations, suggesting that up to 15% CO_2 could be potentially the best blend for running gas turbines under stable operation with moderate swirl numbers.

Acknowledgements

Cardiff University also gratefully acknowledges the support from the Welsh European Funding Office (WEFO) through its program “Flexible Integrated Energy Systems (FLEXIS)”, project no. 80835.

References

[1] Lieuwen T., Torres H., Johnson C., Zinn T., A mechanism of combustion instability in lean premixed gas turbine combustors. *J. Eng. Gas Turbines Power*, 2001, 123(1): 182–190.

[2] Huang Y., Shanwu W., Yang V., *Combustion instabilities in gas turbine engines operational experience, fundamental mechanisms and modeling*, American Institute of Aeronautics and Astronautics Inc., Raston, 2005, pp.: 213–276.

[3] Rayleigh J. W., Rayleigh L., The theory of sound, Dover, New York, 1945.

[4] Durox D., Moeck J., Bourgouin J., Morenton P., Viallon M., Schuller T., Candel S., Flame dynamics of a variable swirl number system and instability control. *Combustion and Flame*, 2013, 160(9):1729–1742.

[5] Candel S., Durox D., Schuller T., Bourgouin J., Moeck J., Dynamics of Swirling Flames CRZ: central recirculation zone. *Annu. Rev. Fluid Mech*, 2014, 46:147–73. DOI:10.1146/annurev-fluid-010313-141300.

[6] Syred N., A review of oscillation mechanisms and the role of the precessing vortex core (PVC) in swirl combustion systems. *Progress in Energy and Combustion Science*. 2006, 32(2): 93-161.

[7] Huang Y., Yang V., Dynamics and stability of lean-premixed swirl-stabilized combustion. *Prog. Energy Combust. Sci.*, 2009, 35(4): 293–364.

[8] Hibshman R., Cohen M., Banaszuk A., Anderson J., Alholm A., Active control of combustion instability in a liquid-fueled sector combustor. *ASME International Gas Turbine and Aeroengine Congress and Exhibition*, 1999, V002T02A030--V002T02A030.

[9] Han X., Li J., Morgans A., Prediction of combustion instability limit cycle oscillations by combining flame describing function simulations with a thermoacoustic network model. *Combustion and Flame*, 2015, 162(10): 3632 - 3647.

[10] Gas turbine with exhaust gas recycle: UKCCSRC pilot-scale advanced capture technology. http://www.pact.ac.uk/facilities/PACT-Core-Facilities/Gas-Turbine/gas-turbine-with-exhaust-gas-recycle-gt-egr/, 2018 (accessed on September 8, 2018).

[11] Lieuwen T., Mcdonell V., Petersen E., Santavicca D., Fuel Flexibility Influences on Premixed Combustor Blowout, Flashback, Autoignition, and Stability. *J Eng Gas Turbines Power*, 2008, 130(1): 011506 (10 pages). DOI: 10.1115/1.2771243.

[12] Richards G., McMillian M., Gemmen R., Rogers W., Cully S., Issues for low-emission, fuel-flexible power systems. *Prog. Energy Combust. Sci.*, 2001, 27(2): 141–169.

[13] Lieuwen T., Mcdonell V., Petersen E., Santavicca D., Fuel Flexibility Influence on Premixed Combustor Blowout, Flashback, Autoignition and Stability. Proceedings of GT2006 ASME Turbo Expo, 2006, Power for Land, Sea and Air GT2006-90770.

[14] Park J., Lee K., Lee E., Effects of CO_2 addition on flame structure in counterflow diffusion flame of $H_2/CO_2/N_2$ fuel. *Int. J. Energy Res.*, 2000, 25. DOI: 10.1002/er.694.

[15] Lewis J., Marsh R., Valera-Medina A., Morris S., Baej H., The use of CO_2 to improve stability and emissions of an IGCC combustor. ASME Turbo Expo:Turbine Technical Conference and Exposition, 2014, p. V04AT04A029--V04AT04A029.

[16] Røkke P., Hustad J., Exhaust gas recirculation in gas turbines for reduction of CO_2 emissions; combustion testing with focus on stability and emissions. *Int. J. Thermodyn.*, 2005, 8(4):167–173.

[17] Herraiz L., Sanchez-Fernandez E., Palfi E., Lucquiad M., Selective exhaust gas recirculation in combined cycle gas turbine power plants with post-combustion CO2 capture. Int J Greenhouse Gas Control, 2018. DOI: 10.1016/j.ijggc.2018.01.017.

[18] Guteza-Bozo M., Valera-Medina A., Syred N., Bowen P.J., Fuel quality impact analysis for practical implementation of corn COB gasification gas in conventional gas turbine power plants. Biomass and Bioenergy. 2019, 122:221-230. DOI: 10.1016/j.biombioe.2019.01.012.

[19] Al-Doboon A., Gutesa M., Valera-Medina A., Syred N., Ng J.H., Chong C.T., CO2-Argon-Steam Oxy-Fuel (CARSOXY) combustion for CCS inert gas atmospheres in gas turbines. Applied Thermal Engineering, 2017, 122: 350-358. DOI: 10.1016/j.applthermaleng.2017.05.032.

[20] Yilmaz H., Yilmaz I., Combustion and emission characteristics of premixed $CNG/H_2/CO/CO_2$ blending synthetic gas flames in a combustor with variable geometric swirl number. Energy, 2019, 172:117-133. DOI: 10.1016/j.energy.2019.01.108

[21] Liu H., Cui Y., Chen B., Kyritsis C., Tang Q., Feng L., Wang Y., Li Z., Geng C., Yao M., Effects of Flame Temperature on PAHs and Soot Evolution in Partially Premixed and Diffusion Flames of a Diesel Surrogate. Energy and Fuels, 2019, 33(11): 11821–11829.

[22] Durox D., Schuller T., Noiray N., Candel S., Experimental analysis of nonlinear flame transfer functions for different flame geometries. *Proc. Combust. Inst.*, 2009, 32(1):1391–1398.

[23] Palies P., Schuller T., Durox D., Candel S., Modeling of premixed swirling flames transfer functions. *Proc. Combust. Inst.*, 2011, 33(2): 2967–2974.

[24] Ducruix S., Schuller T., Durox D., Candel S., Combustion dynamics and instabilities: elementary coupling and driving mechanisms. *J. Propuls. power*, 2003, 19(5): 722–734.

[25] Dowling A., A kinematic model of a ducted flame. *J. Fluid Mech.*, 1999, 394(1): 51–72.

[26] Lieuwen T., Modeling premixed combustion-acoustic wave interactions: A review. *J. Propuls. power*, 2003, 19(5): 765–781.

[27] Armitage C., Balachandran R., Mastorakos E., Cant R., Investigation of the nonlinear response of turbulent premixed flames to imposed inlet velocity oscillations. *Combustion and Flame*, 2006, 146(3):419–436.

[28] Balachandran R., Ayoola B., Kaminski C., Dowling A., Mastorakos E., Experimental investigation of the nonlinear response of turbulent premixed flames to imposed inlet velocity oscillations. *Combustion and Flame*, 2005,143(1):37–55.

[29] Palies P., Durox D., Schuller T., Candel S., Nonlinear combustion instability analysis based on the flame describing function applied to turbulent premixed swirling flames. *Combustion and Flame*, 2011,158(10):1980–1991.

[30] Silva C., Nicoud F., Schuller T., Durox D., Candel S., Combining a Helmholtz solver with the flame describing function to assess combustion instability in a premixed swirled combustor. *Combustion and Flame*, 2013, 160(9):1743–1754.

[31] Dowling P., Nonlinear self-excited oscillations of a ducted flame. *J. Fluid Mech.*, 1997, 346: 271–290. DOI: 10.1017/S0022112097006484.

[32] Dantec Dynamics: BSA Flow Software for LDA. https://www.dantecdynamics.com/download-login, 2018 (accessed on July 15, 2018).

[33] Dantec Dynamics, *StreamWare Basic Installation and User Guide*. https://www.dantecdynamics.com/components/streamware-basic/, 2018 (accessed on July 15, 2018).

[34] Moeck P., Bourgouin F., Durox D., Schuller T., Candel S., Tomographic reconstruction of heat release rate perturbations induced by helical modes in turbulent swirl flames. *Exp. Fluids*, 2013, 54(4): Article No.1498. DOI: 10.1007/s00348-013-1498-2.

[35] Worth A., Dawson R., Tomographic reconstruction of OH* chemiluminescence in two interacting turbulent flames. *Meas. Sci. Technol.*, 2012, 24(2): p. 24013.

[36] Ishino Y., Ohiwa N., Three-dimensional computerized tomographic reconstruction of instantaneous distribution of chemiluminescence of a turbulent premixed flame. *JSME Int. J. Ser. B Fluids Therm. Eng.*, 2005, 48(1):34–40.

[37] Ayoola B., Balachandran R., Frank J., Mastorakos E., Kaminski C., Spatially resolved heat release rate measurements in turbulent premixed flames. *Combustion and Flame*, 2006, 144(1):1–16.

[38] Lieuwen T., Online combustor stability margin assessment using dynamic pressure data. *Trans. ASME-A-Engineering Gas Turbines Power*, 2005, 127(3): 478–482.

[39] Cohen J. M., Proscia W., Delaat J., *Combustion instabilities in gas turbine engines operational experience, fundamental mechanisms and modeling*, American Institute of Aeronautics and Astronautics Inc., Raston, 2005, pp.: 113–145.

[40] Hermann J., Hoffmann S., *Combustion instabilities in gas turbine engines operational experience, fundamental mechanisms and modeling*, American Institute of Aeronautics and Astronautics Inc., Raston, 2005, pp.: 611–634.

[41] Cohen J. M., Banaszuk A., *Combustion instabilities in gas turbine engines operational experience, fundamental mechanisms and modeling*, American Institute of Aeronautics and Astronautics Inc., Raston, 2005, pp.: 581–609.

[42] Sewell J. B., Sobieski P. A., *Combustion instabilities in gas turbine engines operational experience, fundamental mechanisms and modeling*, American Institute of Aeronautics and Astronautics Inc., Raston, 2005, pp.: 147–162.